Holography and speckle in phase-shifting digital holography

Invited Paper

Ichirou Yamaguchi

Toyo Seiki Seisakusyo, 1-2-6 Funado, Itabashi-ku, Tokyo 174-0041, Japan

E-mail: ichiyama1115@yahoo.co.jp

Received August 18, 2009

The correlation properties of the optical field diffusely reflected from a rough surface under coherent illumination are analyzed numerically. The cross-correlations of the complex amplitudes and the intensities before and after translation and/or tilt of the surface are calculated at an arbitrary observation plane in three-dimensional (3D) space. The results provide us with the 3D distributions of phase changes and speckle displacement that lead to the distributions and signal-to-noise ratio of the displacement to be measured by holographic interferometry and speckle correlation technique. Comparisons with analytical relationships and physical interpretation of them are also discussed.

OCIS codes: 030.0030, 090.0090, 120.0120.

doi: 10.3788/COL20090712.1104.

High coherence of laser light opened the new field of interferometry that can be applied to diffusely reflecting surfaces. Holography enables three-dimensional (3D) imaging by recording amplitude and phase of the object wave, while the speckle patterns appearing in the laser scattered by a diffuse surface show high contrast everywhere in 3D space. Holographic interferometry and speckle metrology detect changes of phase and intensity of the light diffusely reflected from diffuse surfaces and are closely related with each other because the changes of intensity and phase are dependent on each other. Localization and interpretation of the fringe patterns observed in holographic interferometry were widely discussed[1−4]. Relationships between holographic interferometry and speckle methods were later clarified analytically[5,6]. These results were utilized in electronic recording and processing of speckle patterns employed for speckle metrology. Digital holography that comprises both digital recording of holograms and digital reconstruction of images brings these techniques even closer to each other because of flexibility of digital recording and processing of intensities obtained from comparatively simple optical setups, realizing automatic and quantitative measurements of surface shape and deformation of 3D diffuse objects. However, the effects of digital recording such as those of number and pitch of charge-coupled device (CCD) pixels and the bit-depth of video signals cannot be investigated in a simple analytic way. Even the optical influence of surface roughness requires complicated assumptions on its interaction with incident light. In this letter, we propose a comparatively simple model based on the random phase scatterers model for an object and the angular spectrum for propagation[7]. It has been employed for computer simulation and is applicable to general problems appearing in the measurement of surface shape and deformation using coherent light.

In the former theory on fringe formation in holographic and speckle interferometry, we expressed the complex amplitude at an observation plane by a linear superposition of the complex amplitude at the object plane[5]. The weighting function for the superposition is either the parabolic wave or the diffraction at a lens aperture, depending on the mutual position of an object and an observation field. The observation field is either the diffraction field or the image field. In the present analysis, the both observation fields can be investigated from the unified standpoint that is based on the angular spectrum expansion of optical fields[7]. We also assume a process of digital holography where the complex amplitude in the diffraction field is recorded and reconstructed to produce an image of the object. In this case, hologram size plays a role of a lens aperture, while the resolution of the CCD limits a size of the recordable object. Thus we can treat the general imaging systems including digital holography and ordinary lens setups.

In digital holography, a laser beam is divided into two paths, a reference and an object, and recombined to generate a hologram as an interference pattern, which is recorded by a CCD and stored in a computer. We start from a digital holographic setup represented by the two-dimensional (2D) coordinate system shown in Fig. 1. A diffuse object is illuminated by a point monochromatic source S with the wave number $k = 2\pi/\lambda$.

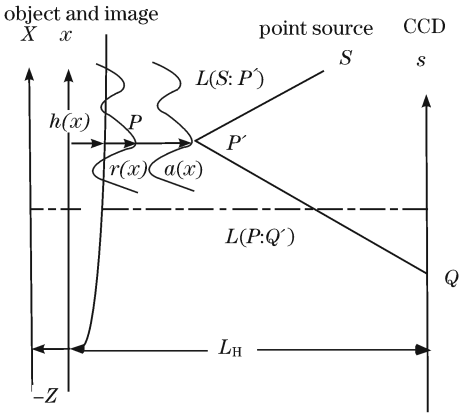

Fig. 1. Coordinate system.

An object point $P[x,\ h(x)+r(x)]$, where $h(x)$ and $r(x)$ mean the initial mean surface and the random roughness profile, respectively, is assumed to be displaced to $P'[x+a_x(x),\ h(x)+r(x)+a_z(x)]$ with the displacement vector $\mathbf{a}(a_x, a_z)$. The complex amplitudes at the CCD plane are represented by superposition of spherical waves scattered by assemblies of object point P or P'. The distribution of $r(x)$ is represented by random numbers uniformly distributed between $(-r_{\rm m}/2,\ r_{\rm m}/2)$, where $r_{\rm m}$ represents the maximum surface roughness. At the hologram plane, the complex amplitude arising from the surface point associated with a sample point x_j at the object plane is added with macroscopic amplitude but with random phase differences introduced by the surface roughness:

$$U(s:a)=\sum_{j=1}^{M}\sqrt{I_{\rm O}(x_j+a_{xj})}\exp\left\{{\rm i}k[L(S:P')+L(P':Q)]\right\},\quad(1)$$

where $I_{\rm O}(x)$ is the macroscopic intensity distribution at the object and

$$L\left(A:B\right)=\sqrt{\left(x_A-x_B\right)^2+\left(z_A-z_B\right)^2}\quad(2)$$

is the distance between the points $A(x_A,z_A)$ and $B(x_B,z_B)$. At the CCD plane distant from the object by $L_{\rm H}$, the complex amplitude is combined with the reference beam having the complex amplitude $U_{\rm R}=A_{\rm R}e^{{\rm i}\delta}$ to yield the intensity

$$I_{\rm H}\left(s:a:\delta\right)=\left|A_{\rm R}\,\exp\left({\rm i}\delta\right)+U\left(s:a\right)\right|^2.\quad(3)$$

Each pixel of the CCD with the pitch p, the width w, and the pixel number N delivers the output

$$S\left(m:a:\delta\right)=\int_{(m-1)p}^{(m-1)p+w}I_{\rm H}\left(s:a:\delta\right){\rm d}s\ \ (m=1-N).\quad(4)$$

In phase-shifting digital holography[8], at least three holograms are recorded after phase shifts of the reference beam. In the case of three-step algorithm, the complex amplitude of the object wave is derived as

$$\begin{aligned}U(m:a)=&\,S(m:a:0)-S(m:a:\pi)\\&+{\rm i}[S(m:a:0)-2S(m:a:\pi/2)\\&+S(m:a:\pi)].\end{aligned}\quad(5)$$

The image reconstruction is conducted by the angular spectrum method. It is appropriate here because of no limitation on the distance between the object and the reconstruction plane as well as the constant sample pitch of the reconstructed image equal to p.

For image reconstruction by the angular spectrum expansion, we first calculate the Fourier transform $\hat{U}(m{:}a)$ of the above derived complex amplitude given by

$$\hat{U}\left(m:a\right)=\sum_{n=1}^{N}U(n:a)\exp\left(-{\rm i}2\pi mn\right),\quad(6)$$

which leads to the complex amplitude at the plane Z from the object calculated as

$$\begin{aligned}U(n,Z:a)=&\sum_{m=1}^{N}\hat{U}(m:a)\\&\exp\left[{\rm i}2\pi\left(nm-(L_{\rm H}-Z)\sqrt{\frac{1}{\lambda^2}-(\frac{m}{Np})^2}\right)\right].\end{aligned}\quad(7)$$

For measurement of surface deformation, we calculate the complex coherence factor defined by an average of the conjugate product of the complex amplitudes before and after object deformation on the reconstruction plane:

$$\begin{aligned}\Gamma(n,Z:a)=&\sum_{m=-M}^{M}U(n+m,Z:0)\\&U^*(n+m,Z:a).\end{aligned}\quad(8)$$

It is a unique advantage of digital holography that we can calculate this coherence factor directly instead of the interference intensity approached in the conventional interferometry. We have recently shown that the phase of the coherence factor is proportional to the object displacement and speckle noise is suppressed more efficiently by this algorithm[9].

We can also derive the speckle displacement at the observation plane from the cross-correlation function of the reconstructed intensity given by

$$C\left(m,\ Z:a\right)=\frac{\sum_{n=1}^{N-m}|U(n,Z:0)|^2|U(n+m,Z:a)|^2}{C(0,Z:a)},\quad(9)$$

whose peak position and height mean speckle displacement and decorrelation due to object deformation, respectively[5]. The fringe pattern in holographic interferometry is visible when the speckle displacement is smaller than the mean speckle size and therefore the axial dependence of speckle displacement governs the fringe localization. At the plane of no speckle displacement with only decorrelation, called speckle boiling, the fringes exhibit the localization.

Phase-shifting digital holography thus provides most directly both the phase change and speckle displacement in the 3D space by recording the complex amplitude at the CCD plane.

The above algorithm is programmed by using Mathematica 5.1 to simulate deformation measurements as well as the surface contouring using dual wavelengths or two sources[10]. Optical systems and CCD specifications for hologram recording can be chosen arbitrarily. Even effects of the recording bit depths and phase-shifting error can also be analyzed. These effects are difficult to investigate analytically.

In the following, we present the results for deformation measurement. The object is a plate with the diameter of 10 mm. The number of object points equally spaced is taken to be 1024. The mean object surface is assumed to be flat and the maximum surface roughness $r_{\rm m}$ is taken to be equal to 10 μm. Object deformation is a tilt about the y-axis Ω_y leading to an out-of-plane displacement given by $a_z=\Omega_y x$. We assume the collimated illumination with the normal

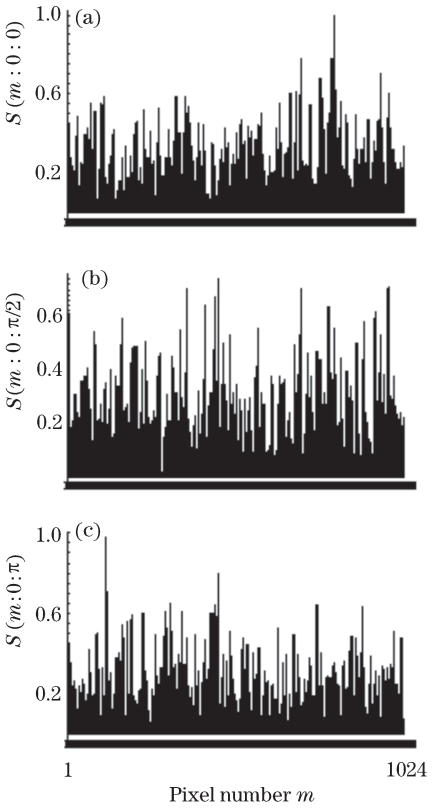

Fig. 2. CCD signals for holograms with phase shift (a) 0, (b) $\pi/2$, and (c) π before object deformation.

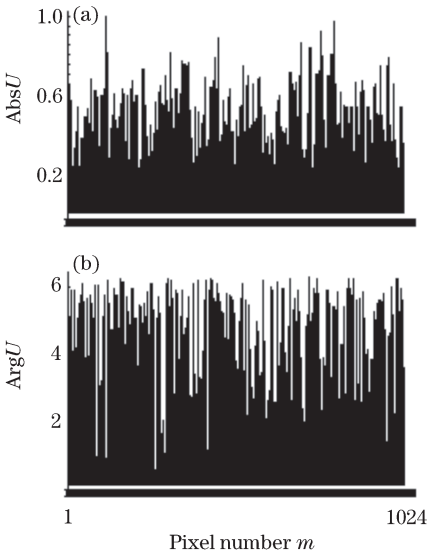

Fig. 3. (a) Amplitude and (b) phase derived from the signals shown in Fig. 2.

incidence and the wavelength 657 nm. No parabolic approximation is employed for the distances between the source and the object and between the object and the observation point. The CCD is located at a distance of $L_{\rm H} = 200$ mm from the object and has the pixels of pitch $p = 5$ μm with a width of photosensitive region $w = 5$ μm and the pixel number $N = 1024$. The CCD outputs resulting from 3 phase-shifted holograms before object deformation given by Eq. (4) are displayed in Fig. 2. These outputs are analyzed by Eq. (5) to derive the amplitude and phase, as shown in Fig. 3.

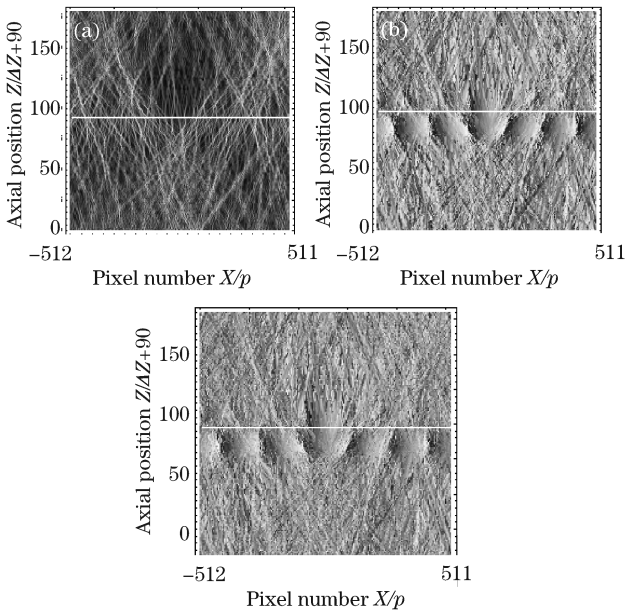

Fig. 4. Distributions of (a) the modulus and phase of the coherence factor (b) before and (c) after averaging.

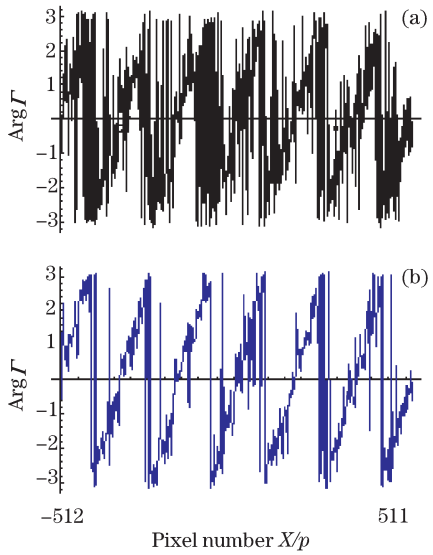

Fig. 5. Cross-section of the coherence factor at the localization plane (a) without and (b) with averaging.

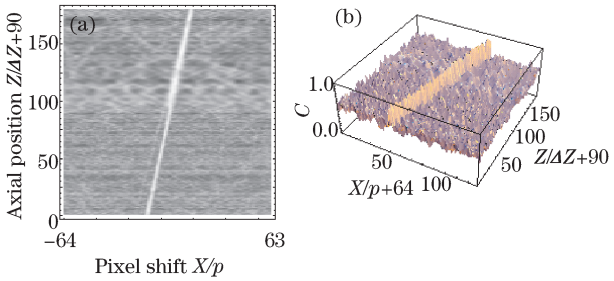

Fig. 6. (a) Density plot and (b) 3D display of the intensity cross-correlation function.

The X-Z distributions of the amplitude and phase of the coherence factor given by Eq. (8) are shown in Fig. 4. The modulus and the phase of the factor without

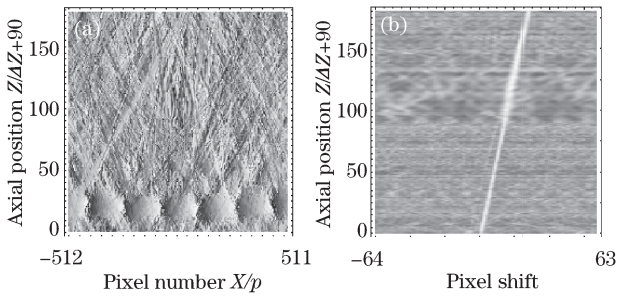

Fig. 7. (a) Phase of the coherence factor and (b) contour of the intensity cross-correlation in the presence of tilt and in-plane translation of the object.

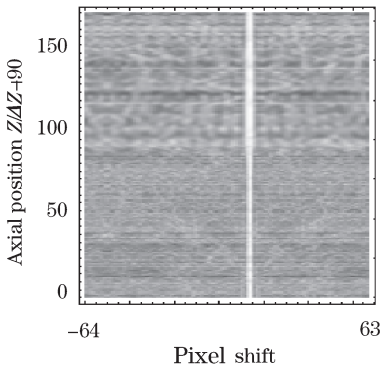

Fig. 8. Intensity cross-correlation due to in-plane translation of the object.

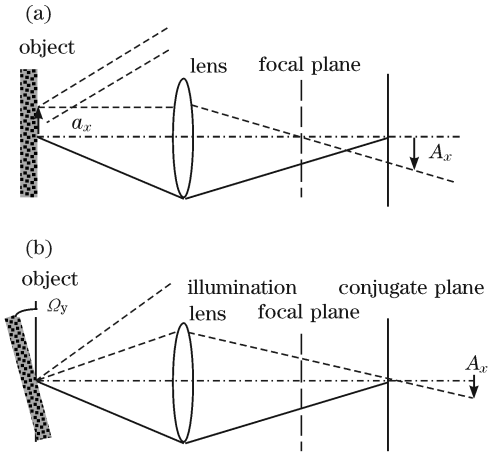

Fig. 9. Axial dependences of speckle displacement due to (a) in-plane translation and (b) tilt of the object.

averaging ($M = 1$) and only the phase of the averaged factor ($M = 3$) are displayed. The scale of X-axis is equal to the sensor pitch 5 μm and that of Z-axis is taken to be the axial speckle size given by $\Delta Z = \lambda(L_{\rm H}/Np)^2$. Analytically, the phase of the averaged coherence factor should be directly proportional to a_z. We note that the phase of the coherence factor exhibits localization at $Z = 0$. The localization should occur at the plane of no speckle displacement and the fringe contrast depends on the ratio of the speckle displacement to the mean speckle size[6]. The depth of the localization is ten times larger than the axial speckle size ΔZ. It depends on the fringe frequency.

The cross-sections of the phases for $M = 1$ and 3 at the localization plane are shown in Fig. 5. We see that the speckle noise is effectively suppressed by the spatial averaging with $M = 3$. The effects of speckle suppression in experiments have been reported before[9].

The speckle displacement is obtained from the peak position of the intensity cross-correlation given by Eq. (9), and the contour is plotted in Fig. 6. Although the correlation computation was carried out by means of one-dimensional (1D) fast Fourier transform (FFT) algorithm using 1024 pixels with the pitch p, only the values for 128 shifts are displayed. The position of the very sharp correlation peak represents speckle displacement and is proportional to Z as predicted by a theory[11]. The speckle displacement actually vanishes at the plane of fringe localization that coincides with the object plane and changes its sign across the plane. The speckle displacement is analytically given by $A_x = 2\Omega_y Z$, that agrees well with the present result.

The localization plane is shifted when an in-plane displacement a_x is added. The amount of shift is given by $S_{\rm L} = a_x/2\Omega_y$. This shift is demonstrated by adding the in-plane translation a_x to the above simulation. The results from $\Omega_y = 0.0004$ rad and $a_x = 0.05$ mm are displayed in Fig. 7, where the phase of the coherence factor with $M = 3$ and the distribution of speckle displacement are shown. Thus the in-plane translation shifts the localization plane and the plane of speckle boiling out of the object plane. The speckle displacement at each plane is increased by an amount equal to the given translation. We also calculate the axial distribution of speckle displacement caused by pure in-plane translation, as shown in Fig. 8. The speckle displacement is equal to the object translation and uniform in space. In this case, no fringe pattern is observed at the observation plane, but in the Fourier plane the fringes of equal inclination are localized that also correspond to the Young fringes observed in speckle photography.

The speckle displacement caused by the tilt and translation of the object under the collimated illumination can be illustrated through Fig. 9. Effects of a lens used in ordinary imaging are also shown. The plane of fringe localization can be used for detection of the surface position[12], but the same measurement can be accomplished from detection of speckle displacement with higher resolution because its axial dependence can be more sensitized by increasing the tilt angle. This corresponds to increasing the spatial frequency of the fringe pattern to reduce the localization depth.

In conclusion, we have reported the method and results for the numerical simulation of deformation measurement of diffuse objects by phase-shifting digital holography. As an advantage of the digital holography over the conventional holographic or speckle interferometry, we can directly calculate the interference term and attain higher signal-to-noise ratio in the measurement. This has proven to be more effective to suppress the speckle noise appearing in phase analysis than simply averaging the phase difference. We can also display the 3D distribution of the complex coherence factor whose phase is directly proportional to the object displacement. This is the background of classical fringe localization phenomenon. It is well known that at the localization position, the speckle displacement is less than the mean speckle size. Axial distribution of speckle displacement derived from

the cross-correlation of the intensities has also been displayed to demonstrate the situation. Thus by comparing these distributions we can measure not only the out-of-plane displacement but also the in-plane translation of the object. Although the localization position for pure tilt of the object provides the surface position without attaching any marking on the surface, the speckle displacement caused by tilt of the object leads to the position more accurately. The results reported here will help us to extract much more information about shape, deformation, and position of diffusely reflecting surfaces by reconstructing 3D distributions of the intensity and the coherence factor of the scattered coherent field.

References

1. S. Walles, Opt. Acta **17,** 899 (1970).
2. N.-E. Molin and K. A. Stetson, Optik **31,** 281 (1970).
3. C. M. Vest, *Holographic Interferometry* (Wiley, New York, 1978).
4. I. Yamaguchi, Opt. Acta **25,** 299 (1978).
5. I. Yamaguchi, "Fringe formations in deformation and vibration measurements using laser light" in E. Wolf, (ed.) *Progress in Optics* Vol.24 (North-Holland, Amsterdam, 1985) p.271.
6. I. Yamaguchi, Opt. Lasers Eng. **39,** 411 (2003).
7. J. A. Ratcliffe, Rep. Prog. Phys. **19,** 188 (1956).
8. I. Yamaguchi and T. Zhang, Opt. Lett. **22,** 1268 (1997).
9. I. Yamaguchi and M. Yokota, Opt. Eng. **48,** 085602 (2009).
10. I. Yamaguchi, T. Ida, M. Yokota, and K. Yamashita, Appl. Opt. **45,** 7610 (2006).
11. I. Yamaguchi, Opt. Acta **28,** 1359 (1981).
12. I. Yamaguchi, T. Ida, and M. Yokota, Strain **44,** 349 (2008).